Molecular cloning and functional characterization of inhibitor-sensitive (mENT1) and inhibitor-resistant (mENT2) equilibrative nucleoside transporters from mouse brain

Andor KISS*, Kalthoum FARAH*, Joon KIM†, Robert J. GARRIOCK†, Thomas A. DRYSDALE† and James R. HAMMOND*[1]

*Department of Pharmacology & Toxicology, M275 Medical Sciences Building, University of Western Ontario, London, Ontario, Canada N6A 5C1, and †Lawson Research Institute, St. Joseph's Health Centre, London, Ontario, Canada N6A 4V2

Mammalian cells express at least two subtypes of equilibrative nucleoside transporters, i.e. ENT1 and ENT2, which can be distinguished functionally by their sensitivity and resistance respectively to inhibition by nitrobenzylthioinosine. The ENT1 transporters exhibit distinctive species differences in their sensitivities to inhibition by dipyridamole, dilazep and draflazine (human > mouse > rat). A comparison of the ENT1 structures in the three species would facilitate the identification of the regions involved in the actions of these cardioprotective agents. We now report the molecular cloning and functional expression of the murine (m)ENT1 and mENT2 transporters. *mENT1* and *mENT2* encode proteins containing 458 and 456 residues respectively, with a predicted 11-transmembrane-domain topology. mENT1 has 88 % and 78 % amino acid identity with rat ENT1 and human ENT1 respectively; mENT2 is more highly conserved, with 94 % and 88 % identity with rat ENT2 and human ENT2 respectively. We have also isolated two additional distinct cDNAs that encode proteins similar to mENT1; these probably represent distinct mENT1 isoforms or alternative splicing products. One cDNA encodes a protein with two additional amino acids (designated mENT1b) that adds a potential protein kinase CK2 phosphorylation site in the central intracellular loop of the transporter, and is similar, in this regard, to the human and rat ENT1 orthologues. The other cDNA has a 5′-untranslated region sequence that is distinct from that of full-length mENT1. Microinjection of mENT1, mENT1b or mENT2 cRNA into *Xenopus* oocytes resulted in enhanced uptake of [^{3}H]uridine by the oocytes relative to that seen in water-injected controls. mENT1-mediated, but not mENT2-mediated, [^{3}H]uridine uptake was inhibited by nitrobenzylthioinosine and dilazep. Dipyridamole inhibited both mENT1 and mENT2, but was significantly more effective against mENT1. Adenosine inhibited both systems with a similar potency, as did a range of other purine and pyrimidine nucleosides. These results are compatible with the known characteristics of the native mENT1 and mENT2 transporters.

Key words: dipyridamole, nitrobenzylthioinosine, nucleoside transport, transporter isoforms, *Xenopus* oocytes.

INTRODUCTION

Pharmacological manipulation of the extracellular and intracellular levels of nucleosides (both endogenous and synthetic analogues) has been investigated in relation to a number of clinical situations. These include enhancement of the target selectivity and effectiveness of cytotoxic nucleoside analogues used in anti-cancer and anti-viral therapy [1,2], as well as manipulation of the biological activities of adenosine to enhance its neuroprotective [3–7] and cardioprotective [8–12] actions. Many of these protocols involve inhibition of the cellular uptake or release of nucleosides. Hydrophilic nucleosides, such as adenosine, do not readily cross cell membranes by passive diffusion [13]. Their transfer into and out of cells is mediated by two distinct families of nucleoside transporter proteins: Na^+-independent equilibrative transporters and Na^+-dependent concentrative transporters [14–16]. These transporters are also essential for the salvage of nucleosides for nucleotide and nucleic acid synthesis, particularly in cell types that lack the ability to synthesize nucleosides *de novo* [17,18]. Based on functional analyses of radiolabelled nucleoside flux in cultured cells, six subtypes of Na^+-dependent concentrative transporters (N1–N6) and two subtypes of equilibrative transporters have been identified [15]. The present study focused on the equilibrative transporters. These systems are widely expressed in many different cell lines and tissues, and they play a major role in cellular permeability to endogenous nucleosides and nucleoside analogues.

The two equilibrative, Na^+-independent, transporters are defined by their differential sensitivities to nitrobenzylthioinosine (NBMPR) [15,16]. The '*es*' (**e**quilibrative inhibitor-**s**ensitive) transporter is blocked by concentrations of NBMPR lower than 1 nM, whereas concentrations in excess of 1 μM are required to inhibit the '*ei*' (**e**quilibrative inhibitor-**i**nsensitive) transporter. The *es* transporter is also more sensitive than the *ei* transporter to other inhibitors, such as dilazep, dipyridamole and draflazine [16,19,20]. However, unlike that seen using NBMPR, the actual potency of these latter compounds for inhibiting the *es* transporter is very species-dependent [21–26]. Dipyridamole, for example, has a K_i of approx. 10 nM for inhibiting the human *es* transporter, whereas the mouse *es* transporter exhibits a K_i of

Abbreviations used: *ei*, equilibrative inhibitor-insensitive nucleoside transport; ENT, equilibrative nucleoside transporter (the prefixes m, r and h denote mouse, rat and human respectively); *es*, equilibrative inhibitor-sensitive nucleoside transport; EST, expressed sequence tag; GSP, gene-specific primer; NBMPR, nitrobenzylthioinosine {6-[(4-nitrobenzyl)thio-9-β-D-ribofuranosylpurine}; PKC, protein kinase C; RACE, rapid amplification of cDNA ends; RT-PCR, reverse transcriptase–PCR; TM, transmembrane segment; UTR, untranslated region.

[1] To whom correspondence should be addressed (e-mail jhammo@julian.uwo.ca).

The nucleotide sequence data reported will appear in the GenBank®, EMBL, GSDB and DDBJ Nucleotide Sequence Databases under the following accession numbers: mENT1, AF131212; mENT2, AF183397; mENT1b, AF305501.

© 2000 Biochemical Society

approx. 100 nM and the rat *es* transporter is very resistant to inhibition by dipyridamole, with a K_i value greater than 10 μM. cDNAs have been derived from human and rat tissues that, when expressed in *Xenopus* oocytes, encode proteins with functional and pharmacological characteristics typical of the *es* and *ei* nucleoside transporters [27–30]. These cDNAs have been designated ENT1 (*es* phenotype) and ENT2 (*ei* phenotype), and the encoded proteins are predicted to have 11 transmembrane segment (TM) domains with a cytoplasmic N-terminus. The ENT proteins are members of a newly discovered gene family, with no similarity to any other mammalian substrate transporters for which there are molecular data. The ENT1 and ENT2 designations will be used to refer to the equilibrative transporter subtypes for the remainder of this paper.

To facilitate the development of more subtype-selective nucleoside transport inhibitors for use as clinical modifiers of adenosine bioactivity, it will be necessary to gain a better understanding of the structural differences between transporter subtypes and species orthologues that give rise to their distinctive pharmacology. We now report the molecular cloning of the mouse ENT1 (mENT1) and mENT2 transporters. The availability of these cDNAs, along with those for the rat and human orthologues, will enable detailed structure–function studies to be carried out, in order to delineate the defining ligand–protein interactions underlying the affinity and selectivity of nucleoside transport inhibitors and substrates.

EXPERIMENTAL

In brief, partial cDNAs encoding proteins with a high degree of sequence similarity to the human ENT1 (hENT1; *es*) and hENT2 (*ei*) transporters were isolated by reverse transcriptase–PCR (RT-PCR) amplification of poly(A^+)-selected mRNA isolated from CD-1 mouse whole-brain tissue. Additional sequence data were then obtained by 5′- and 3′-RACE (rapid amplification of cDNA ends), using gene-specific primers designed from the RT-PCR products. The full-length cDNA clones for mENT1 and mENT2 were obtained by RT-PCR using primers based on the 5′- and 3′-RACE products.

mENT1

The initial primers for RT-PCR amplification of mENT1 were derived from the EST (expressed sequence tag) sequences w59610 and aa397253. These ESTs were identified through a search of the mouse EST database at the National Centre for Biotechnology Information using hENT1 (accession no. u81375) as the query sequence. The sense primer corresponded to nucleotide positions 12–32 of mEST w59610 (5′-AACCTCCTGCCTGAGCCTGAG-3′), and the antisense primer corresponded to nucleotide positions 383–403 of mEST aa397253 (5′-CTGGCAGGGAAGGAAGTGAGC-3′). *Taq* polymerase (Life Technologies, Burlington, ON, U.S.A.) was used in the initial studies to optimize the PCR conditions; all subsequent studies used the proof-reading Advantage cDNA PCR Polymerase mix from Clontech (Palo Alto, CA, U.S.A.). First-strand cDNA synthesis was performed on 1 μg of mRNA template using the BRL SuperScript® PreAmplification System (Life Technologies) with an oligo$(dT)_{12–18}$ primer. PCR reactions were performed in a Thermocycler PE 480 (Perkin Elmer, Norwalk, CT, U.S.A.) using an oil-overlaid 50 μl reaction mixture in thin-walled 500 μl reaction tubes, and products were resolved by electrophoresis on a 1% (w/v) agarose gel. Amplification parameters were as follows: (a) 94 °C for 3 min (one cycle); (b) 94 °C for 1 min, 59 °C for 1 min and 72 °C for 2 min (30 cycles); and (c) 72 °C for 10 min. A single amplicon product of ~ 1500 bp was obtained, gel-purified, ligated into the TA-cloning vector pGEM-T (Promega, Madison, WI, U.S.A.) and subcloned into DH5α *Escherichia coli* competent cells (Life Technologies) using standard procedures. The plasmid inserts were sequenced with a *Taq* BigDye Terminator Cycle Sequencing Kit using an automated ABI PRISM Model 377 Version 3.3 DNA Sequencer (PE Applied Biosystems, Norwalk, CT, U.S.A.). This process identified two distinct cDNA sequences (50:50 ratio in six clones sequenced) with open reading frames encoding proteins with greater than 80% sequence identity with hENT1. These two mENT1 isoforms differed in the absence (mENT1a) or the presence (mENT1b) of two additional amino acids and a flanking arginine-to-serine substitution in the large central intracellular loop (predicted), which effectively introduced an additional protein kinase CK-2 interaction site in mENT1b (see Figures 1 and 2). Both mENT1a and mENT1b were also cloned from murine Ehrlich ascites tumour cells.

The remaining 5′-untranslated region (5′-UTR) and 3′-UTR sequence data for mENT1 were obtained from mouse brain using 5′- and 3′-RACE. The gene-specific primer (GSP) for 5′-RACE was 5′-GTCCCCACAGGGTCACACAAGTGCCC-3′, corresponding to nt 1520–1545 of mENT1a, and the GSP for 3′-RACE was 5′-GGGGCCTGCAGAGCAAGAGACCAAGT-3′, corresponding to nt 873–898 of mENT1a. The complementary primer was the AP1 oligonucleotide provided by Clontech, designed to hybridize with the Clontech RACE Adaptor. PCR reaction parameters were based on the manufacturer's (Clontech) recommended parameters for touch-down, two-step PCR. The first set of parameters were: (a) five cycles at 94 °C for 30 s and 72 °C for 4 min; (b) five cycles at 94 °C for 30 s and 70 °C for 4 min; and (c) 25 cycles at 94 °C for 20 s and 66 °C for 4 min. The secondary PCR reaction used the AP2 primer (Clontech) and the GSP used in the first reaction with similar parameters, except that the number of cycles was reduced, to three cycles in steps (a) and (b) each and to 19 cycles in (c). The amplicon produced by this method (1400 bp) was purified and prepared for sequencing as described above. The ENT1 3′-RACE amplicon was also obtained by two-step PCR. The primary reaction was carried out as per the manufacturer's recommendations, with the exception that the number of cycles in the amplification step was reduced to 20, and 69 °C was used as the annealing/extension temperature. The secondary PCR utilized both the AP2 primer (Clontech) and a nested GSP, 5′-ATTGGGTTGTTCCCTGCT-3′, corresponding to nt 1060–1077 of mENT1a. The reaction parameters for the secondary PCR were: (a) 94 °C for 30 s and 72 °C for 1 min (two cycles); (b) 94 °C for 30 s and 70 °C for 1 min (two cycles); and (c) 94 °C for 20 s and 68 °C for 2 min (16 cycles), which resulted in a single amplicon of 1030 bp. These RACE products were ligated into pGEM-T and sequenced as described above. The full-length mENT1 cDNA was then obtained by RT-PCR amplification of poly$(A)^+$-selected mRNA isolated from CD-1 mouse whole-brain tissue using primers designed to the 5′- and 3′-ends of the 5′-RACE and 3′-RACE products respectively (sense primer, 5′-TTGAGTGGTCCTGAGTCTGCAGAGGCT-3′; antisense primer, 5′-AATCAGATGGCCTCTGAAGGCACCTGG-3′), and the following reaction conditions: (a) 94 °C for 1 min to denature; and (b) 94 °C for 30 s, 66 °C for 1 min and 72 °C for 4 min (40 cycles). The resulting mENT1 amplicon (2031 bp) was ligated into pGEM-T and sequenced in both directions. The mENT1 cDNA had an open reading frame encoding a 458-residue protein flanked by 187 bp of untranslated 5′-nucleotide sequence and 452 bp of untranslated 3′-sequence. The open reading frame of the full-length mENT1 cDNA was identical with that of mENT1a (as

© 2000 Biochemical Society

opposed to mENT1b). However, mENT1a differed from the full-length mENT1 in the first 95 nt of untranslated 5′-nucleotide sequence (see Figure 3).

mENT2

The coding region of mENT2 was obtained by RT-PCR using a sense primer designed to the 5′-end of the rat ENT2 (rENT2; accession no. af015305) open reading frame (5′-GCGGACATCATGGCGCACGGAAA-3′) and an antisense primer to the 3′-end of mHNP36 (accession no. x86682) (5′-GTGGAGGATTCTTCCTCACCATATGC-3′). mHNP36 was identified in a screen of the GenBank® database with hENT2 (GenBank® accession no. AF02358) as the query sequence. PCR amplification was performed as described above for mENT1, but with the following changes: (a) 94 °C for 3 min (one cycle); (b) 94 °C for 1 min, 59 °C for 1 min and 72 °C for 1 min (40 cycles with a segment extension of 1 s per cycle); and (c) 72 °C for 10 min. This PCR reaction generated a 1529 bp product that was ligated into pGEM-T and prepared for sequencing as described above. This procedure was repeated three times with two distinct first-strand cDNA preparations, resulting in clones with identical nucleotide sequences, designated $mENT2_{5R}$ (the 5R signifies the 5′ 21 nt from rENT2).

The true 5′-end of the mENT2 coding region, as well as the remaining 5′- and 3′-UTR sequences, were then obtained using RACE, similar to that described above for mENT1. For mENT2, the 5′-RACE GSP was 5′-GTGAACGTCCCAACTCCAGAA-GCTGCAC-3′, corresponding to nt 1414–1441 of $mENT2_{5R}$, and the GSP for 3′-RACE was 5′-TCCCGTACTTCCAGGG-GCGGTTAG-3′, corresponding to nt 116–139 of $mENT2_{5R}$. The PCR reaction was performed by touch-down, two-step PCR as described above (using a 68 °C annealing/extension temperature). The 3′-RACE product resolved as a single band of ~2100 bp on 1% (w/v) agarose gels. However, the initial 5′-RACE procedure resulted in multiple products. To obtain a single 5′-RACE product for mENT2, a second, semi-nested, PCR reaction with the AP2 primer (Clontech) was required using the manufacturer's recommended parameters as detailed above. This reaction produced an approx. 1150 bp product that was ligated into pGEM-T and sequenced. The full-length mENT2 cDNA was then obtained by RT-PCR amplification of poly(A)$^+$-selected mRNA isolated from CD-1 mouse whole-brain tissue using primers designed to the RACE products (sense primer, 5′-GCAGTGTAACCCAACCCCGACCCTCCGCTA-3′; antisense primer, 5′-GAACAGTTTTAATTGGATGCAGGAGC-AGGG-3′) with the following reaction conditions: (a) 94 °C for 1 min to denature; and (b) 94 °C for 30 s, 66 °C for 1 min and 72 °C for 4 min (40 cycles). The resulting mENT2 amplicon (2372 bp) was ligated into pGEM-T and sequenced in both directions. The mENT2 cDNA had an open reading frame encoding a 456-residue protein flanked by 153 bp of untranslated 5′-nucleotide sequence and 851 bp of untranslated 3′-sequence, and was identical with the partial sequences obtained by 5′- and 3′-RACE and $mENT2_{5R}$ (with the exception of the first 21 nucleotides of $mENT2_{5R}$ that correspond to rENT2).

Expression in *Xenopus* oocytes

Plasmids containing the mENT1 and mENT2 inserts were linearized using *Sph*I and transcribed with either SP6 or T7 polymerase (depending on the directionality in the plasmid) in the presence of ^{m7}GpppG cap using the mMessage mMachine (Ambion, Austin, TX, U.S.A.) *in vitro* transcription kit. Capped RNA size was checked on a 1% Mops/formaldehyde denaturing gel and quantified by spectroscopic analysis. *Xenopus laevis* female frogs were pithed and the ovary lobes were removed, segmented and placed in ND96 medium (96 mM NaCl, 2 mM KCl, 1 mM $MgCl_2$, 1 mM $CaCl_2$, 5 mM Hepes and 2.5 mM pyruvate, pH 7.5) supplemented with gentamicin sulphate (50 μg/ml) and BSA (0.1%, w/v). Follicular cells were removed from the oocytes by manual dissection, and the defolliculated oocytes were incubated overnight at 18 °C in ND96 medium supplemented with 0.1% BSA and 50 μg/ml gentamicin sulphate. Oocytes were then injected with 10 nl of double-distilled water alone (control) or containing mENT1 or mENT2 RNA transcript (1 ng/nl) using a Drummond Nanoject Auto Injector (Drummond Scientific Co., Broomall, PA, U.S.A.). ND96 medium was changed twice daily, with oocytes being incubated for 48–72 h at 18 °C prior to use in functional assays.

[^{3}H]Uridine uptake assays

The uptake of 10 μM [^{3}H]uridine (10 μCi/ml) by *Xenopus* oocytes was assessed using a method similar to that described by Young and co-workers [30,31]. Between ten and twelve oocytes were pooled for each assay condition in a final incubation volume of 0.2 ml. After a defined incubation time, oocytes were washed rapidly six times with 1 ml of ice-cold buffer (ND96, without supplements); individual oocytes were then digested overnight in 5% (w/v) SDS, and the ^{3}H content of each oocyte was assessed by standard liquid scintillation procedures. For inhibition studies, competing unlabelled nucleoside substrates were added concurrently with the [^{3}H]uridine, and inhibitors such as NBMPR and dipyridamole were incubated with the oocytes for approx. 15 min before addition of [^{3}H]uridine. A 5 min uptake time was chosen for the inhibition studies, based on the results of the uptake time course profiles, which showed that the rate of uptake of [^{3}H]uridine was linear up to this time point (see Figure 4). Assays using oocytes injected with double-distilled water and RNA were conducted in parallel. Likewise, oocytes injected with mENT1 and mENT1b RNAs were assessed in parallel.

Results for the uptake experiments are given as means ± S.E.M. for 20–30 individual oocytes. Non-linear curve fitting to the data was performed using Prism (v 3.0) software (GraphPAD, San Diego, CA, U.S.A.). Each experiment was performed at least two times using oocytes from different animals.

RESULTS AND DISCUSSION

Functional studies of the uptake of radiolabelled nucleosides by mammalian cells have identified a heterogeneous population of equilibrative nucleoside transporters that differ widely in their pharmacological properties [15,16]. Many cells express both NBMPR-sensitive and NBMPR-resistant transporters, and these two functional phenotypes have recently been correlated with the existence of two distinct gene products, designated ENT1 and ENT2 respectively [27–30]. Our laboratory has conducted extensive studies on the functional and pharmacological characteristics of the mENT1 and mENT2 transporters expressed by Ehrlich ascites tumour cells [20,32,33]. The mENT1 transporter has an affinity for dipyridamole (K_i ~100 nM) that is intermediate between those of the hENT1 and rENT1 transporters. This suggests that there are multiple structural determinants for dipyridamole binding to the transporter, and that the mouse transporter shares at least one additional interaction site for dipyridamole with the human transporter that is not found in rENT1. We have also screened a variety of analogues of draflazine and have identified functional groups important for ENT1 versus ENT2 selectivity in the mouse, as well as chemical features that contribute to hENT1 versus mENT1 binding affinity [20,34]. These structure–activity data, in conjunction with the amino acid

© 2000 Biochemical Society

sequences of mENT1 and mENT2 determined in the present study, will assist in the delineation of the protein domains involved in the binding of draflazine, and other cardioprotective agents, to nucleoside transporters [11,35,36].

mENT1

The full-length mENT1 cDNA, obtained by RT-PCR using primers designed from the 3′- and 5′-RACE products, encoded a 458-residue protein (M_r 50076) (Figure 1) that was 88 % identical (93 % similar) with rENT1 and 78 % identical (86 % similar) with hENT1 in amino acid sequence. Hydropathy analysis predicted an eleven-TM-domain topology for mENT1, with a cytoplasmic N-terminus (Figure 2), similar to those of hENT1 and rENT1 [27,28,30]. Notably, mENT1 was similar to hENT1 in that it did not contain the additional cysteine residue that is found in the fourth extracellular loop of rENT1. However, mENT1 had a four-amino-acid insert (Arg-His-His-Phe) in the fifth extracellular loop that was not found in either hENT1 or rENT1. Relative to hENT1, mENT1 was also missing two amino acids (Lys-Gly) from the large central intracellular loop; however, another mENT1 isoform (mENT1b; Figure 1 and see below) was also identified in the present study that did not have this particular two-amino-acid deletion. In general, the major differences in ENT1 sequence between species (rat, mouse and human) occurred in the C-terminal half of the large extracellular loop between TM1 and TM2 and in the fifth extracellular loop between TM9 and TM10; these differences may contribute to the distinctive affinities of the transporters from the three species for the cardioprotective agents dipyridamole, dilazep and draflazine [21–26,34]. In this regard, Sundaram et al. [37] have used hENT1/rENT1 chimaeric constructs to identify a region bordered by residues 100 and 231 in hENT1 as being critical for the interaction of dipyridamole and dilazep with the transport protein. However, in the same study, a construct containing residues 1–99 of hENT1 and residues 100–457 of rENT1 encoded a protein that retained partial sensitivity to dipyridamole, indicating that interactions with the hydrophilic loop between TM1 and TM2 may also be involved in the binding reaction. It is noteworthy that the amino acid sequence between residues 99 and 231 is highly conserved between species (Figure 2), suggesting that differences in dipyridamole sensitivity may be due to discrete amino acid substitutions in this region. Structure–activity studies [19,34,38] have led to the hypothesis that interactions with discrete hydrophobic elements of the transporter are required for high-affinity binding of inhibitors to hENT1. Comparative hydropathy analysis showed that residues 50–67 of the first extracellular loop of hENT1 are significantly more hydrophobic than the corresponding residues in mENT1 and rENT1; indeed, this region is the only one that displays a marked difference in hydrophobicity among the species examined. This part of the first extracellular loop may, therefore, contribute to the binding of the species-discriminating transport inhibitors, such as dipyridamole and some draflazine analogues [34].

mENT1, like hENT1, has a single putative glycosylation site in the first extracellular loop (Asn-48). This coincides with the finding that photoaffinity-labelled mENT1 transporters migrate on SDS/polyacrylamide gels with an apparent M_r of 45000 [39], which is close to the size of the hENT1 transporter (M_r 45000–55000) but much smaller than the rENT1 transporter ($M_r \sim 62000$), which has three potential glycosylation sites [40]. This glycosylated residue has been implicated in the binding of NBMPR to hENT1, as mutation of this residue to glutamine resulted in a 10-fold decrease in the affinity of NBMPR for the mutant transporter expressed in yeast [41]. We have also noted that partial deglycosylation of mouse Ehrlich cell membranes with endoglycosidase F significantly decreased the binding of [^{3}H]NBMPR to these membranes (J. R. Hammond and M. Su, unpublished work).

Interestingly, two distinct mENT1 isoforms (mENT1a and mENT1b) were obtained by RT-PCR using primers based on the mouse ESTs w59610 and aa397253. The peptide encoded by mENT1b differed from that encoded by mENT1a and the full-length mENT1 by an Arg-254 → Ser substitution and a two-amino-acid insert (Lys-Gly) after residue 254 (Figures 1 and 2). These modifications insert a potential protein kinase CK2 phosphorylation site into the sequence, raising the possibility that these isoforms may be subject to differential regulation by phosphorylation. Preliminary data from our laboratory suggest that inhibition of protein kinase CK2 activity does lead to an up-regulation of hENT1 activity in osteosarcoma cells (L. Cooper, G. Vilk, D. W. Litchfield and J. R. Hammond, unpublished work). ESTs have been identified in the GenBank® database that correspond to both of these mENT1 isoforms, confirming their physiological expression. Two ESTs, both derived from a day-7.5 post-conception mouse embryo cDNA library (accession nos. AA407561 and AA409415), corresponded to mENT1b (containing the sequence encoding the CK2 site), while three ESTs were found (AU051703, AW320820 and AA270375; each isolated from different libraries) with the characteristic six-base deletion of mENT1a. It is noteworthy that the hENT1 and rENT1 sequences that have been reported previously are most similar to the mENT1b isoform.

mENT1, like the rat and human orthologues, also has two potential protein kinase C (PKC) phosphorylation sites in the intracellular hydrophilic loops (Figure 2): one near the C-terminal end of the region joining TM2 and TM3 (Ser-109) and one in the large intracellular loop between TM6 and TM7 (Thr-274). Although direct phosphorylation of the transporters by PKC has not yet been demonstrated, PKC activators (i.e. phorbol esters) have been shown to down-regulate nucleoside transport activity in neural cells [42], HL60 leukaemia cells [43,44], human B-lymphocytes [45] and cultured chromaffin cells [46].

The present study also provides preliminary evidence for the existence of two distinct 5′-UTR sequences associated with mENT1. The mENT1 sequences (mENT1a/b) obtained using the EST-derived primers had a distinct 5′-UTR sequence relative to the full-length mENT1 obtained using primers designed to the 5′-and 3′-RACE products (Figure 3). Six EST sequences (accession nos. AI047867, W59610, AA237136, AW321734, AW647617 and AI451844) were identified in the GenBank® database that corresponded to the 5′-UTR of mENT1a/b. Only one EST sequence (accession no. AU051152; M. Sasaki, Y. Suzuki, M. Watanabe, J. Imai, A. Shibui, K. Yoshida, H. Hata, R. Yamaguchi, S. Tateyama and S. Sugano) was found that contained a 5′-UTR corresponding to that of the full-length mENT1 cDNA derived via 5′- and 3′-RACE; notably, this latter EST was also derived from brain tissue. It is not yet known if these two 5′-UTRs are indicative of multiple gene products or alternative splicing products derived from a single gene.

mENT2

The full-length mENT2 cDNA encoded a 456-residue protein (M_r 50255) that was 94 % identical (95 % similar) with rENT2 and 88 % identical (92 % similar) with hENT2 in amino acid sequence, with a predicted topography (Figure 2) similar to that determined for mENT1. Compared with mENT1, mENT2 was notable in the high degree of conservation of amino acid sequence between species (Figure 2) and, with the exception of the loop

© 2000 Biochemical Society

Figure 1 Alignment of the predicted amino acid sequences of mENT1 and mENT2

Amino acid sequences were deduced from the nucleotide open reading frames for each clone. A shaded background denotes residues that are identical in mENT1 and mENT2. The residues that distinguish the mENT1b isoform are indicated above the mENT1 sequence (white letters on a black background). The bars above and below the sequences represent the predicted transmembrane regions of mENT1 and mENT2 respectively.

connecting TM1 and TM2, in the relatively short extracellular connecting loops between the predicted TM α-helices. mENT2 was similar to rENT2 in that it lacked the glycine residue that is present at position 46 of hENT2, and had a threonine insert at position 315 (Thr-316 in rENT2) and a lysine insert at position 246 (Lys-247 in rENT2). However, mENT2 differed from rENT2 in having a serine insert at position 227 (Ser-228 in hENT2), and it differed from both rENT2 and hENT2 in the deletion of two amino acids (Ser-270 and Glu-271 of hENT2) from the intracellular loop joining TM6 and TM7, as well as in the addition of a glutamine residue in position 358 of mENT2. There are two N-linked glycosylation sites in the first extracellular loop (Asn-47 and Asn-56) and a potential protein kinase CK2 phosphorylation site in the third intracellular loop (Thr-236). In addition, as noted for mENT1, there is a PKC consensus sequence in the first intracellular loop (Ser-95) and another in the large third intracellular loop (Thr-223), indicating that mENT2 may also be subject to regulation by PKC-mediated phosphorylation.

The primary functional difference between the ENT1 and ENT2 transporters in mouse cells is the lower affinity of ENT2 for inhibitors of nucleoside transport, such as NBMPR, dilazep and draflazine [20]. At the amino acid level, mENT1 and mENT2 are 47% identical (70% similar; see Figure 1). The greatest differences are in the extracellular hydrophilic loops and the large intracellular domain joining TM6 and TM7. In particular, the extracellular loop between TM1 and TM2 of mENT1 has 14 additional residues relative to mENT2 (Figure 1). The fifth extracellular loop joining TM9 and TM10 of mENT2 is also missing four amino acids found in mENT1, and is poorly conserved in the remaining residues of the loop (Figure 1). It is noteworthy that these two loops in ENT1 are also the ones that show the greatest variability between species (Figure 2). The reduced size of the first and fifth extracellular loops of mENT2 compared with mENT1 is offset by the presence of a larger (+15 residues) intracellular loop between TM6 and TM7, resulting in the similar protein sizes of mENT1 and mENT2. The 15-residue insert in the intracellular loop of mENT2 is also notable in that it includes a proline-rich region that meets the minimum requirements for SH3 (Src homology 3) domain interactions [47,48].

A search of the GenBank® database revealed 12 entries with similarity to mENT2. The most significant match was with mHNP36 (accession no. X86682), which corresponds to positions 345–2372 of mENT2 (99% identity). mHNP36 was identified as a mitogen-activated, delayed/early response gene that encodes a nucleolar protein [49]. Three alternative splice isoforms of the human homologue of HNP36 have been identified that encode related, but distinct, proteins [50]. These data suggest that mENT2 encodes a transporter that participates in the uptake/release of nucleosides by intracellular organelles. In this regard, there is recent functional evidence for the expression of both hENT1 and hENT2 in intracellular compartments of BeWo cells [51]. In addition to mHNP36, a further 11 mouse ESTs were identified (AW542486, AW537215, C79114, AA675457, AI851366, AW060591, AV375781, AV248983, AV104874, AV301231 and AV230133). All of the ESTs indicated were similar to the 3′-end of mENT2 (downstream of nt 1763) and were generally derived from embryonic or neonatal tissues.

After the initial submission of the present study for publication, sequences corresponding to mENT1, mENT1b and mENT2 were deposited in the GenBank® database by Dr A. Gordon and colleagues at the Gallo Research Institute (San Francisco, CA, U.S.A.). These cDNA sequences were derived from the hybrid NG108-15 mouse neuroblastoma × rat glioma cell line, with the two ENT1 isoforms designated as mENT1.1 (accession no.

© 2000 Biochemical Society

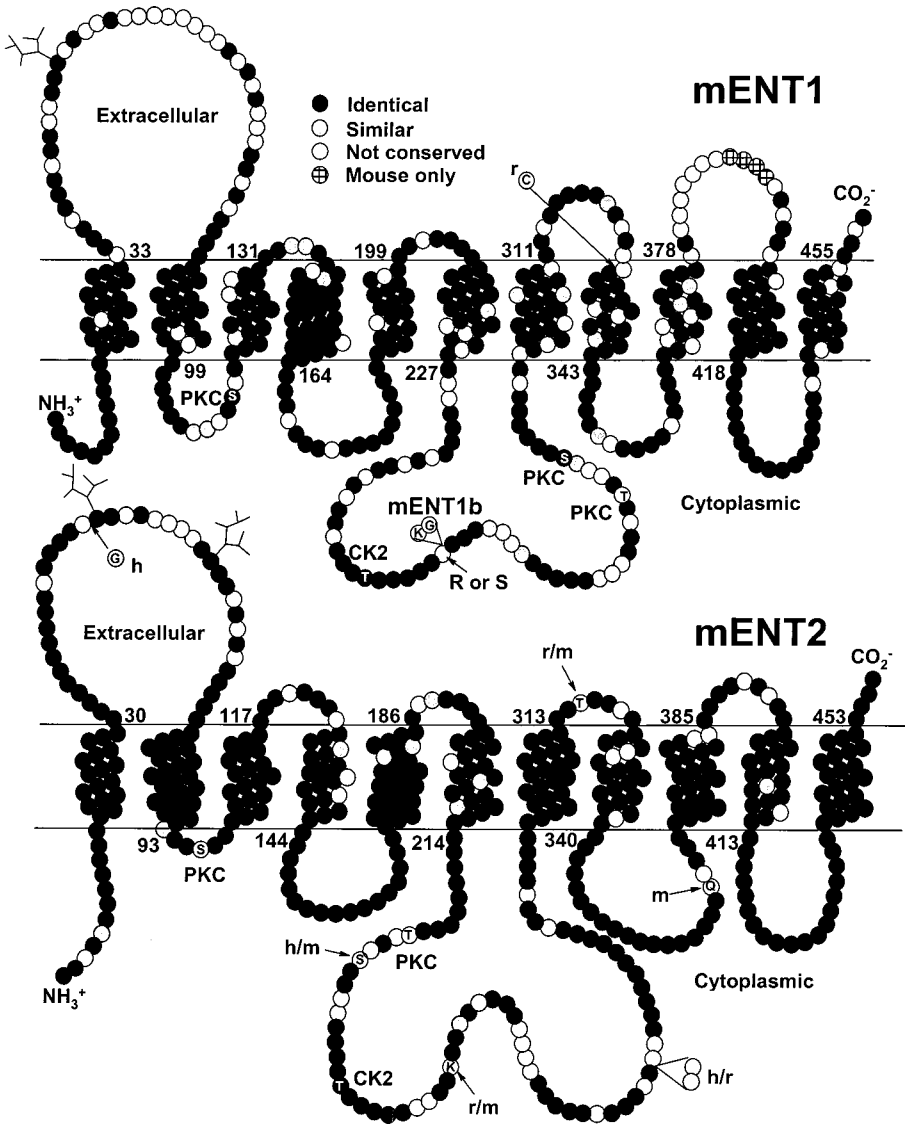

Figure 2 Topological model of mENT1 and mENT2: comparison with rat and human homologues

Potential membrane-spanning regions and orientation were determined with the TMpred program (http://www.ch.embnet.org/software/TMPRED_form.html). Potential N-linked glycosylation sites are indicated by 'branching lines', and putative serine/threonine phosphorylation sites are indicated by the associated protein kinase (PKC or protein kinase CK2). Residues identical with those found in both the human and rat homologues are shown as black circles; conservative substitutions in all three species are shown as grey circles. Residues that are not conserved in at least one of the other species are shown as white circles. Residues missing from the mouse sequence that are found in other species are indicated along with the first letter of the species in which the insertion is found. Residues found in the mouse sequence that are missing from either the rat or human sequence are indicated with an arrow along with the first letter of the species in which this residue is found. Note that there are four amino acids in the fifth extracellular loop of mENT1 that are not found in either hENT1 or rENT1. The two-amino-acid insertion in the third intracellular loop of mENT1b is also indicated, along with the serine substitution for Arg-254 of mENT1.

AF257188) and mENT1.2 (accession no. AF257189), corresponding to mouse brain mENT1b and mENT1 respectively. The mENT1.1 sequence is missing the first 95 nucleotides of mENT1b, and differs from mENT1b at five other positions along the sequence. mENT1.2 is missing the first 132 bases of brain mENT1, and differs at three other positions along the sequence. It is noteworthy that the 5′-UTR that is missing from both mENT1.1 and mENT1.2 is the variable region located upstream of nucleotide 133 of the mouse brain mENT1 identified in the present study (see Figure 3). Mouse brain mENT2 has an additional 41 bases at the 5′-end and 15 bases at the 3′-end compared with the NG108-15 mENT2 (accession no. AF257190). The two mENT2 transcripts also differ at six other discrete points along the nucleotide sequence. These nucleotide differences may reflect the fact that the cDNAs isolated in the present study were derived from normal brain tissue, as opposed to a transformed hybrid cell line. The predicted amino acid sequences, however, are identical for mENT1/mENT1.2, mENT1b/mENT1.1 and mENT2 from each source.

Functional expression of mENT1 and mENT2 in *Xenopus* oocytes

The functionality of the proteins encoded by the mENT1, mENT1b and mENT2 cDNA clones was tested by the expression of cRNA, obtained by *in vitro* transcription of the respective cDNA, in *Xenopus* oocytes. This expression system has been

© 2000 Biochemical Society

```
         1 . . . . . . . . . 10. . . . . . . . . 20. . . . . . . . . 30. . . . . . . . . 40. . . . . . . . . 50
mENT1    T T G A G T G G T C C T G A G T C T G C A G A G G C T T C C C T T G C C T A C T C T G T G T C C A G
mENT1a/b - - - - - - - - - - - - - - - - - - - - - - - - - - - - - - - - - - - - - - A A C C T C C T G C C T G A G C

         . . . . . . . . . 60. . . . . . . . . 70. . . . . . . . . 80. . . . . . . . . 90. . . . . . . . . 100
mENT1    C T C T A C C C C C C C C C C C C A A G A G A A A G G C C C A G G G C A G T G T G G A A G C A G A
mENT1a/b C T G A G C C A G G A C C C C T T C C T G G G G A A C G C C C A G G T A C C T T T G G C T C T C A -

         . . . . . . . . . 110. . . . . . . . . 120. . . . . . . . . 130. . . . . . . . . 140. . . . . . . . . 150
mENT1    G C C A G A C A G G G C T C G A T A T T C C T T T A C C C C C A G C A A G A G C C A G A G G G A G G
mENT1a/b - C C G T C C T G C C A A C A T C G A G T C T A T A A A T T T - G C A A G A G C C A G A G G G A G G
```

Figure 3 mENT1 5′-UTR heterogeneity

Two distinct cDNAs corresponding to mENT1 were obtained, depending on the specific 5′-primer used in the PCR reaction. The cDNA clone designated mENT1 was obtained using a primer designed from the 5′-end of the 5′-RACE product, as described in the text. An alternative 5′-UTR sequence (mENT1a/b) was obtained when using a 5′-primer designed against EST w59610 from Soares mouse embryo. Nucleotides that are identical in the two sequences are indicated by a shaded background; note that sequence identity starts at nt 133, which is 55 bases upstream of the start of the coding region (nt 188). For clarity, only the first 150 nucleotides of the mENT1 sequence are shown.

used successfully for the functional evaluation of the proteins encoded by the human and rat ENT1 and ENT2 cDNAs [27,30]. Oocytes injected with 10 ng of mENT1 RNA transcript accumulated [^{3}H]uridine (10 μM) at a significantly greater rate (0.78 ± 0.07 pmol/5 min per oocyte) than those injected with water alone (0.13 ± 0.01 pmol/5 min per oocyte) (Figure 4). Interestingly, when 10 ng of cRNA prepared from the mENT1b clone was injected into *Xenopus* oocytes, a significantly lower level of expression of [^{3}H]uridine uptake activity was observed (0.34 ± 0.03 pmol/5 min per oocyte; Figure 4) relative to that seen for mENT1. It is unlikely that the two-amino-acid insert in the central intracellular loop of mENT1b contributed to this lower activity, since both the hENT1 and rENT1 transporters have a similar insert in this region, and they have been shown to be functional when expressed in *Xenopus* oocytes [27,30]. It is possible that the difference in the 5′-UTR of mENT1 compared

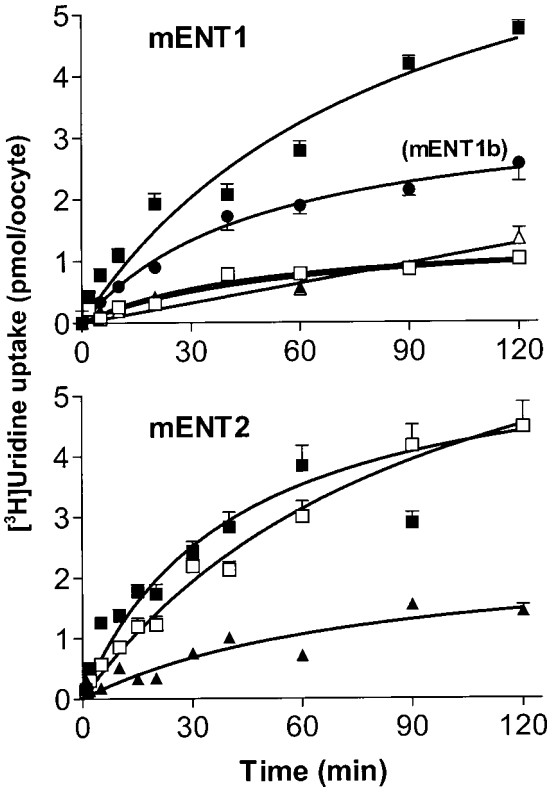

Figure 4 [^{3}H]Uridine uptake by recombinant mENT1 and mENT2 expressed in *Xenopus laevis* oocytes

Oocytes were injected with 10 nl of double-distilled water containing 10 ng of mENT1 (■, □; upper panel), mENT1b (●) or mENT2 (■, □; lower panel) RNA transcript. The uptake of 10 μM [^{3}H]uridine was assessed at room temperature (~ 20 °C) after a 48–72 h incubation of the injected oocytes at 18 °C. Incubation times with [^{3}H]uridine ranged from 1 to 120 min, in the absence (closed symbols) or the presence (open symbols) of 10 μM NBMPR/dipyridamole. Uptake by water-injected oocytes (▲, △) was assessed in parallel with that of the RNA-injected oocytes. The 'zero-time' uptake of [^{3}H]uridine, which was subtracted from all data, was estimated at ~ 2 °C using the minimum possible incubation time (< 10 s). Each value is the mean ± S.E.M. for 20–30 oocytes from at least two independent experiments.

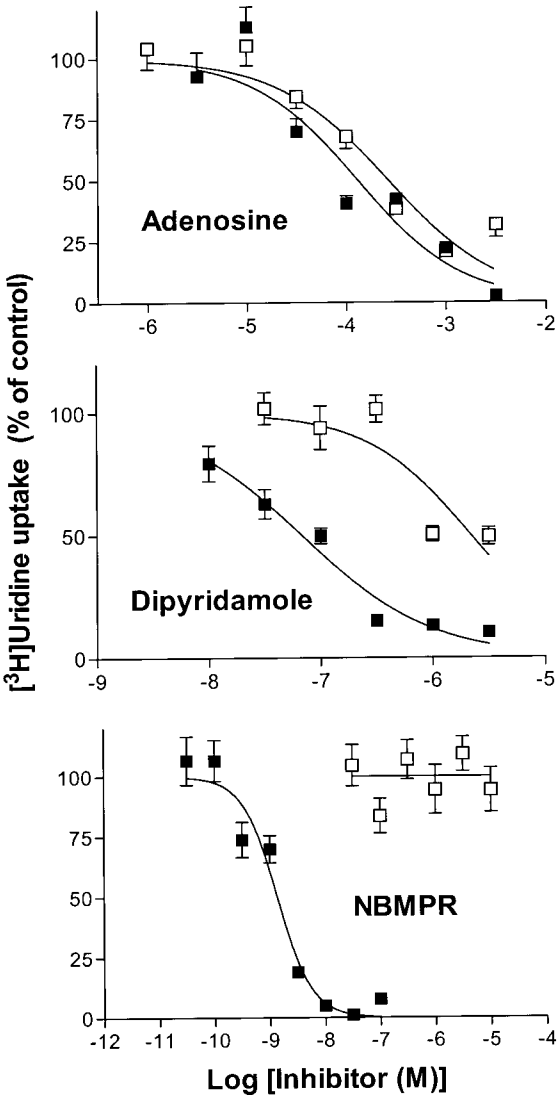

Figure 5 Inhibition of mENT1- and mENT2-mediated uptake of [^{3}H]uridine

Oocytes injected with mENT1 (■) or mENT2 (□) RNA were incubated with 10 μM [^{3}H]uridine for 5 min at ~ 20 °C in the presence or the absence of the indicated concentrations of inhibitors. Oocytes were preincubated for at least 15 min with NBMPR or dipyridamole before the addition of [^{3}H]uridine. Adenosine was added to the oocytes 10 s before the addition of [^{3}H]uridine. The amount of uptake of [^{3}H]uridine by water-injected oocytes was subtracted from all data, and the amount of mENT1/mENT2-mediated uptake is shown as a percentage of that observed in the absence of inhibitor (control). Each value is the mean ± S.E.M. for 20–24 oocytes from two independent experiments.

© 2000 Biochemical Society

Table 1 Inhibition of recombinant and native mENT1- and mENT2-mediated [^{3}H]uridine uptake

IC_{50} values (with 95% confidence intervals in parentheses) for the inhibition of uridine uptake by recombinant mENT1- and mENT2-injected oocytes were calculated from the data shown in Figure 5 by non-linear regression analysis. The K_i values (means ± S.E.M.; $n = 5$) for inhibition of [^{3}H]uridine uptake by the ENT1 and ENT2 transporters of mouse Ehrlich ascites tumour cells were derived from [20].

	Inhibition of mENT1		Inhibition of mENT2	
Inhibitor (units of concn.)	Oocytes (IC_{50})	Ehrlich cells (K_i)	Oocytes (IC_{50})	Ehrlich cells (K_i)
NBMPR (nM)	1.4 (0.8–2.3)	0.16 ± 0.03	> 10000	16000 ± 3000
Dipyridamole (nM)	75 (36–158)	66 ± 17	2204 (481–10100)	371 ± 36
Adenosine (μM)	131 (46–373)	47 ± 2	265 (109–644)	61 ± 7

with that of mENT1b may impact on the stability or translation efficiency of the cRNA in *Xenopus* oocytes. Preincubation of the mENT1-RNA-injected oocytes with 5 μM NBMPR and 5 μM dipyridamole reduced the rate of uptake of [^{3}H]uridine to levels similar to that seen in water-injected oocytes (0.07 ± 0.01 pmol/5 min per oocyte). Incubation of the mENT1-RNA-injected oocytes with a range of concentrations of NBMPR and dipyridamole prior to incubation with 10 μM [^{3}H]uridine for 5 min resulted in the inhibition profiles shown in Figure 5. Analyses of these data yielded IC_{50} values for NBMPR and dipyridamole of 1.4 nM and 75 nM respectively (Table 1). Similar studies involving concurrent incubation of the oocytes with a range of concentrations of adenosine and 10 μM [^{3}H]uridine for 5 min generated an IC_{50} value of 131 μM for adenosine inhibition of mENT1-mediated uptake. These values are very similar to those determined for inhibition by NBMPR, dipyridamole and adenosine of the uptake of 10 μM uridine by the ENT1 transporter of mouse Ehrlich cells (Table 1). The lower affinity of adenosine for the mENT1 transporter expressed in oocytes, relative to that seen in Ehrlich cells, may reflect metabolism of adenosine over the 5 min incubation period in these studies; the previous studies in Ehrlich cells involved a much shorter (20 s) uptake time. Uridine uptake by the oocytes injected with mENT1 RNA was also inhibited by dilazep and by a range of purine and pyrimidine transporter substrates, but not by the nucleobase adenine (Figure 6). These results indicate that the cDNA designated mENT1 in the present study encodes a protein with characteristics compatible with the inhibitor-sensitive subtype (*es*) of the equilibrative nucleoside transporter.

Oocytes injected with mENT2 RNA (10 ng) also accumulated 10 μM [^{3}H]uridine at a significantly greater rate (1.26 ± 0.09 pmol/5 min per oocyte) than water-injected control oocytes (0.18 ± 0.01 pmol/5 min per oocyte) (Figure 4). However, unlike the mENT1-RNA-injected oocytes, the enhanced uptake by the mENT2-injected oocytes could not be inhibited by NBMPR, even at concentrations as high as 20 μM, and was only partially inhibited by dipyridamole at concentrations greater than 1 μM (Figure 5, Table 1). mENT2 was also insensitive to inhibition by 1 μM dilazep. Adenosine, on the other hand, was an effective inhibitor of [^{3}H]uridine uptake by the mENT2-injected oocytes (IC_{50} 265 μM; Figure 5, Table 1), as were other nucleoside substrates, including cytidine, guanosine, thymidine, 2-deoxyadenosine and inosine (Figure 6). Interestingly, 1 mM adenine also produced a small, but significant, inhibition of mENT2, but did not block mENT1-mediated uridine uptake (Figure 6). This pharmacological profile for mENT2-injected *Xenopus* oocytes is compatible with the operation of the inhibitor-resistant subtype (*ei*) of the mouse equilibrative nucleoside transporter (see Table 1).

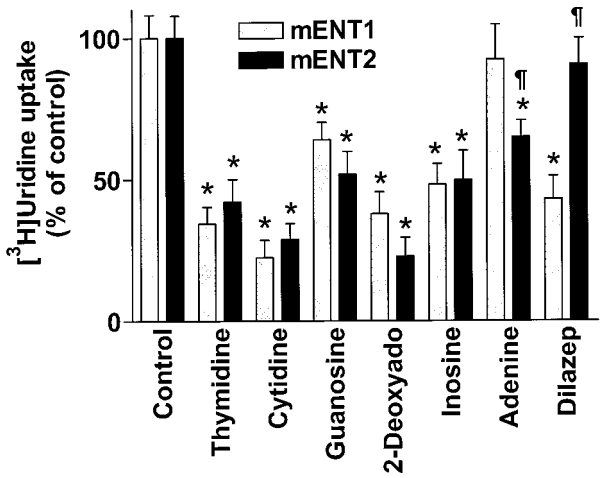

Figure 6 Inhibition of [^{3}H]uridine uptake by transporter substrates and inhibitors

Oocytes injected with mENT1 (hatched bars) or mENT2 (solid bars) RNA (10 ng) were incubated with 10 μM [^{3}H]uridine for 5 min at ~ 20 °C in the presence or the absence (Control) of the indicated inhibitors. Thymidine (1 mM), guanosine (300 μM), cytidine (1 mM), inosine (1 mM), 2-deoxyadenosine (2-Deoxyado; 1 mM) or adenine (1 mM) was added to the assay 10 s before the [^{3}H]uridine. Oocytes were incubated with dilazep (1 μM) for at least 15 min before the assay. Uptake of [^{3}H]uridine by water-injected oocytes, assayed in parallel, was subtracted from all data. Data are shown as percentages of the uptake observed in the absence of inhibitor (Control). Each value is the mean ± S.E.M. of 20–24 oocytes from two independent experiments. Significance of differences: *, significantly different from control; ¶, significantly different from the corresponding mENT1-mediated uptake (randomized-block ANOVA followed by the Student–Newman–Keuls multiple-range test; $P < 0.05$).

Conclusions

In summary, we have isolated cDNAs that encode proteins with the functional and pharmacological characteristics of the mouse inhibitor-sensitive (*es*; mENT1) and inhibitor-resistant (*ei*; mENT2) equilibrative nucleoside transporters. We have also isolated additional cDNA transcripts for mENT1 that differ in their 5′-UTR sequences and in the expression of a potential protein kinase CK2 phosphorylation site in the central intracellular loop. Additional studies will be required to assess the significance of these mENT1 isoforms, but they may represent a novel mode of regulation of ENT1 transporter activity in cells. The availability of ENT1 and ENT2 nucleotide sequences from human, mouse and rat, representing a range of inhibitor sensitivities, will now allow detailed structure–function studies to

© 2000 Biochemical Society

be carried out, in order to assess the interaction of inhibitors with these transport systems. Such information will ultimately assist in the development of more specific nucleoside transport inhibitors and substrates for potential use in chemotherapy and in the treatment of cardiovascular disorders and pathological conditions of neuronal hyperexcitability.

Note added in proof (received October 11, 2000)

Subsequent to the final submission of this manuscript, the mouse ENT1 genomic nucleotide sequence was released to the GenBank® database (accession no. AF218255). Comparative sequence analyses suggest that the three mENT1 cDNA sequence variants reported herein are alternative splicing products of this mENT1 gene.

These studies were supported by grants to J. R. H. and T. A. D. from the Medical Research Council of Canada. K. F. was supported by a Medical Research Council of Canada Studentship.

REFERENCES

1 Mackey, J. R., Baldwin, S. A., Young, J. D. and Cass, C. E. (1998) Nucleoside transport and its significance for anticancer drug resistance. Drug Resist. Updates **1**, 310–324

2 Belt, J. A., Marina, N. M., Phelps, D. A. and Crawford, C. R. (1993) Nucleoside transport in normal and neoplastic cells. Adv. Enzyme Regul. **33**, 235–252

3 Farinelli, S. E., Greene, L. A. and Friedman, W. J. (1998) Neuroprotective actions of dipyridamole on cultured CNS neurons. J. Neurosci. **18**, 5112–5123

4 Deckert, J., Morgan, P. F. and Marangos, P. J. (1988) Adenosine uptake site heterogeneity in the mammalian CNS? Uptake inhibitors as probes and potential neuropharmaceuticals. Life Sci. **42**, 1331–1345

5 Geiger, J. D. and Fyda, D. (1991) Adenosine transport in the CNS. In Adenosine in the Nervous System (Stone, T., ed.), pp. 1–23, Academic Press, San Diego

6 Marangos, P. J. and Miller, L. (1991) Adenosine-based therapeutics in neurologic disease. In Adenosine and Adenine Nucleotides as Regulators of Cellular Function (Phillis, J. W., ed.), pp. 413–422, CRC Press, Ann Arbor

7 Von Lubitz, D. K. J. E., Carter, M. F., Beenhakker, M., Lin, R. C. S. and Jacobson, K. A. (1995) Adenosine: A prototherapeutic concept in neurodegeneration. Ann. N. Y. Acad. Sci. **765**, 163–178

8 Mubagwa, K., Mullane, K. and Flameng, W. (1996) Role of adenosine in the heart and circulation. Cardiovasc. Res. **32**, 797–813

9 Ely, S. W. and Berne, R. M. (1992) Protective effects of adenosine in myocardial ischemia. Circulation **85**, 893–904

10 Abd-Elfattah, A. S., Jessen, M. E., Lekven, J. and Wechsler, A. S. (1998) Differential cardioprotection with selective inhibitors of adenosine metabolism and transport: role of purine release in ischemic and reperfusion injury. Mol. Cell. Biochem. **180**, 179–191

11 Rongen, G. A., Smits, P., Ver, D. K., Willemsen, J. J., De Abreu, R. A., Van Belle, H. and Thien, T. (1995) Hemodynamic and neurohumoral effects of various grades of selective adenosine transport inhibition in humans. Implications for its future role in cardioprotection. J. Clin. Invest **95**, 658–668

12 Van Belle, H. (1993) Nucleoside transport inhibition: a therapeutic approach to cardioprotection via adenosine? Cardiovasc. Res. **27**, 68–76

13 Arch, J. R. S. and Newsholme, E. A. (1978) The control of the metabolism and the hormonal role of adenosine. Essays Biochem. **14**, 82–123

14 Baldwin, S. A., Mackey, J. R., Cass, C. E. and Young, J. D. (1999) Nucleoside transporters: molecular biology and implications for therapeutic development. Mol. Med. Today **5**, 216–224

15 Cass, C. E., Young, J. D. and Baldwin, S. A. (1998) Recent advances in the molecular biology of nucleoside transporters of mammalian cells. Biochem. Cell Biol. **76**, 761–770

16 Griffith, D. A. and Jarvis, S. M. (1996) Nucleoside and nucleobase transport systems of mammalian cells. Biochim. Biophys. Acta Rev. Biomembr. **1286**, 153–181

17 Staub, M., Sasvari-Szekely, M., Solymossy, M. and Szikla, K. (1995) Nucleoside transport and metabolism in lymphocytes, polymorphonuclear cells and cerebral synaptosomes. Adv. Exp. Med. Biol. **370**, 769–774

18 Murray, A. W. (1971) The biological significance of purine salvage. Annu. Rev. Biochem. **40**, 811–826

19 Buolamwini, J. K. (1997) Nucleoside transport inhibitors: structure-activity relationships and potential therapeutic applications. Curr. Med. Chem. **4**, 35–66

20 Hammond, J. R. (1991) Comparative pharmacology of the nitrobenzylthioguanosine-sensitive and -resistant nucleoside transport mechanisms of Ehrlich ascites tumor cells. J. Pharmacol. Exp. Ther. **259**, 799–807

21 Baer, H. P., Haq, A., el Soofi, A., Serignese, V. and Paterson, A. R. (1990) Potencies of mioflazine and its derivatives as inhibitors of adenosine transport in isolated erythrocytes from different species. J. Pharm. Pharmacol. **42**, 367–369

22 Hammond, J. R. and Clanachan, A. S. (1985) Species differences in the binding of [^{3}H]nitrobenzylthioinosine to the nucleoside transport system in mammalian central nervous system membranes: evidence for interconvertible conformations of the binding site/transporter complex. J. Neurochem. **45**, 527–535

23 Ogbunude, P. O. J. and Baer, H. P. (1990) Competition of nucleoside transport inhibitors with binding of 6-[(4-nitrobenzyl)-mercapto]purine ribonucleoside to intact erythrocytes and ghost membranes from different species. Biochem. Pharmacol. **39**, 1199–1204

24 Plagemann, P. G. W. and Woffendin, C. (1988) Species differences in sensitivity of nucleoside transport in erythrocytes and cultured cells to inhibition by nitrobenzylthioinosine, dipyridamole, dilazep, and lidoflazine. Biochim. Biophys. Acta **969**, 1–8

25 Shank, R. P. and Baldy, W. J. (1990) Adenosine transport by rat and guinea pig synaptosomes: basis for differential sensitivity to transport inhibitors. J. Neurochem. **55**, 541–550

26 Griffith, D. A., Conant, A. R. and Jarvis, S. M. (1990) Differential inhibition of nucleoside transport systems in mammalian cells by a new series of compounds related to lidoflazine and mioflazine. Biochem. Pharmacol. **40**, 2297–2303

27 Griffiths, M., Yao, S. Y., Abidi, F., Phillips, S. E., Cass, C. E., Young, J. D. and Baldwin, S. A. (1997) Molecular cloning and characterization of a nitrobenzylthioinosine-insensitive (ei) equilibrative nucleoside transporter from human placenta. Biochem. J. **328**, 739–743

28 Griffiths, M., Beaumont, N., Yao, S. Y. M., Sundaram, M., Boumah, C. E., Davies, A., Kwong, F. Y. P., Coe, I., Cass, C. E., Young, J. D. and Baldwin, S. A. (1997) Cloning of a human nucleoside transporter implicated in the cellular uptake of adenosine and chemotherapeutic drugs. Nature Med. **3**, 89–93

29 Crawford, C. R., Patel, D. H., Naeve, C. and Belt, J. A. (1998) Cloning of the human equilibrative, nitrobenzylmercaptopurine riboside (NBMPR)-insensitive nucleoside transporter *ei* by functional expression in a transport-deficient cell line. J. Biol. Chem. **273**, 5288–5293

30 Yao, S. Y., Ng, A. M., Muzyka, W. R., Griffiths, M., Cass, C. E., Baldwin, S. A. and Young, J. D. (1997) Molecular cloning and functional characterization of nitrobenzylthioinosine (NBMPR)-sensitive (es) and NBMPR-insensitive (ei) equilibrative nucleoside transporter proteins (rENT1 and rENT2) from rat tissues. J. Biol. Chem. **272**, 28423–28430

31 Huang, Q.-Q., Harvey, C. M., Paterson, A. R. P., Cass, C. E. and Young, J. D. (1993) Functional expression of Na^+-dependent nucleoside transport systems of rat intestine in isolated oocytes of *Xenopus laevis*. Demonstration that rat jejunum expresses the purine-selective system N1 (*cif*) and a second, novel system N3 having broad specificity for purine and pyrimidine nucleosides. J. Biol. Chem. **268**, 20613–20619

32 Hammond, J. R. (1992) Differential uptake of [^{3}H]guanosine by nucleoside transporter subtypes in Ehrlich ascites tumour cells. Biochem. J. **287**, 431–436

33 Burke, T., Lee, S., Ferguson, P. J. and Hammond, J. R. (1998) Interaction of 2′,2′-difluorodeoxycytidine (gemcitabine) and formycin B with the Na^+-dependent and -independent nucleoside transporters of Ehrlich ascites tumor cells. J. Pharmacol. Exp. Ther. **286**, 1333–1340

34 Hammond, J. R. (2000) Interaction of a series of draflazine analogues with equilibrative nucleoside transporters: species differences and transporter subtype selectivity. Naunyn Schmiedebergs Arch. Pharmacol. **361**, 373–382

35 Böhm, M., Weinhold, C., Schwinger, R. H., Muller-Ehmsen, J., Böhm, D., Reichenspurner, H., Reichart, B. and Erdmann, E. (1994) Studies of the nucleoside transporter inhibitor, draflazine, in the human myocardium. Br. J. Pharmacol. **112**, 137–142

36 Flameng, W., Sukehiro, S., Mollhoff, T., Van Belle, H. and Janssen, P. (1991) A new concept of long-term donor heart preservation: nucleoside transport inhibition. J. Heart Lung Transplant. **10**, 990–998

37 Sundaram, M., Yao, S. Y., Ng, A. M., Griffiths, M., Cass, C. E., Baldwin, S. A. and Young, J. D. (1998) Chimeric constructs between human and rat equilibrative nucleoside transporters (hENT1 and rENT1) reveal hENT1 structural domains interacting with coronary vasoactive drugs. J. Biol. Chem. **273**, 21519–21525

38 Paul, B., Chen, M. F. and Paterson, A. R. (1975) Inhibitors of nucleoside transport. A structure-activity study using human erythrocytes. J. Med. Chem. **18**, 968–973

39 Hammond, J. R. and Johnstone, R. M. (1989) Solubilization and reconstitution of a nucleoside-transport system from Ehrlich ascites-tumour cells. Biochem. J. **262**, 109–118

40 Kwong, F. Y. P., Wu, J.-S. R., Shi, M. M., Fincham, H. E., Davies, A., Henderson, P. J. F., Baldwin, S. A. and Young, J. D. (1993) Enzymic cleavage as a probe of the molecular structures of mammalian equilibrative nucleoside transporters. J. Biol. Chem. **268**, 22127–22134

© 2000 Biochemical Society

41 Vickers, M. F., Mani, R. S., Sundaram, M., Hogue, D. L., Young, J. D., Baldwin, S. A. and Cass, C. E. (1999) Functional production and reconstitution of the human equilibrative nucleoside transporter (hENT1) in Saccharomyces cerevisiae. Interaction of inhibitors of nucleoside transport with recombinant hENT1 and a glycosylation-defective derivative (hENT1/n48q). Biochem. J. **339**, 21–32

42 Miras-Portugal, M. T., Delicado, E. G., Casillas, T. and Sen, R. P. (1991) Control of nucleoside transport in neural cells. Effect of protein kinase C activation. Adv. Exp. Med. Biol. **309A**, 435–438

43 Lee, C. W., Sokoloski, J. A., Sartorelli, A. C. and Handschumacher, R. E. (1991) Induction of the differentiation of HL-60 cells by phorbol 12-myristate 13-acetate activates a Na^+-dependent uridine-transport system. Involvement of protein kinase C. Biochem. J. **274**, 85–90

44 Lee, C.-W. (1994) Decrease in equilibrative uridine transport during monocytic differentiation of HL-60 leukaemia: involvement of protein kinase C. Biochem. J. **300**, 407–412

45 Soler, C., Felipe, A., Mata, J. F., Casado, F. J., Celada, A. and Pastor-Anglada, M. (1998) Regulation of nucleoside transport by lipopolysaccharide, phorbol esters, and tumor necrosis factor-alpha in human B-lymphocytes. J. Biol. Chem. **273**, 26939–26945

46 Delicado, E. G., Sen, R. P. and Miras-Portugal, M. T. (1991) Effects of phorbol esters and secretagogues on nitrobenzylthioinosine binding to nucleoside transporters and nucleoside uptake in cultured chromaffin cells. Biochem. J. **279**, 651–655

47 Mayer, B. J. and Eck, M. J. (1995) SH3 domains. Minding your p's and q's. Curr. Biol. **5**, 364–367

48 Musacchio, A., Saraste, M. and Wilmanns, M. (1994) High-resolution crystal structures of tyrosine kinase SH3 domains complexed with proline-rich peptides. Nat. Struct. Biol. **1**, 546–551

49 Williams, J. B. (1995) A mammalian delayed-early response gene encodes HNP36. a novel, conserved nucleolar protein. Biochem. Biophys. Res. Commun. **213**, 325–333

50 Williams, J. B., Rexer, B., Sirripurapu, S., John, S., Goldstein, R., Phillips, III, J. A., Haley, L. L., Sait, S. N., Shows, T. B., Smith, C. M. and Gerhard, D. S. (1997) The human HNP36 gene is localized to chromosome 11q13 and produces alternative transcripts that are not mutated in multiple endocrine neoplasia, type 1 (MEN I) syndrome. Genomics **42**, 325–330

51 Mani, R. S., Hammond, J. R., Marjan, J. M., Graham, K. A., Young, J. D., Baldwin, S. A. and Cass, C. E. (1998) Demonstration of equilibrative nucleoside transporters (hENT1 and hENT2) in nuclear envelopes of cultured human choriocarcinoma (BeWo) cells by functional reconstitution in proteoliposomes. J. Biol. Chem. **273**, 30818–30825

Received 5 June 2000/4 August 2000; accepted 15 September 2000

© 2000 Biochemical Society